Ultra-low loss and fabrication tolerant silicon nitride (Si_3N_4) (de-)muxes for 1-μm CWDM optical interconnects

Stanley Cheung, Michael R. T. Tan
Hewlett-Packard Laboratories, 1501 Page Mill Road, Palo Alto, CA. 94304, USA
Author e-mail address: stanley.cheung@hpe.com

Abstract: Low-loss, fabrication-tolerant Si_3N_4 CWDM lattice filters and AWGs are demonstrated for 990 – 1065nm bottom-emitting VCSELs. Channel separation of 25 nm, *XT* < -35 dB and -20 dB are reported with temperature shift of 14.5 pm/°C.

OCIS code: (130.3120) Integrated optics devices; (130.7408) Wavelength filtering devices

1. Introduction

We propose a hybrid optical transceiver that includes a transmitter with VCSELs (990 – 1065 nm) optically coupled to a Si_3N_4 (de-)multiplexer as shown in Fig. 1 (a). After multiplexing the different signals from each VCSEL into a waveguide, launching optics are provided to launch the output from each on-chip single-mode multiplexer into the lowest - order mode group in MMF fiber or the lowest order mode in a SMF fiber. The 3 main desired requirements for the (de-)multiplexer should be: 1) lowering the optical losses such that there is minimal impact on the optical power budget, 2) the pass-band wavelengths are tolerant enough to accommodate high temperature operation (80 °C) such that electrical thermal tuning is not required, 3) the material platform and design is robust enough to yield devices with repeatable performance such that post fabrication trimming is avoided. The cascaded MZI lattice filters and AWGs are fabricated on the 4” Ligentec AN150 platform which consists of a 150 nm LPCVD Si_3N_4 waveguide core layer. The taped-out chip and wafer uniformity map is shown in Fig. 1 (b) and (c) respectively.

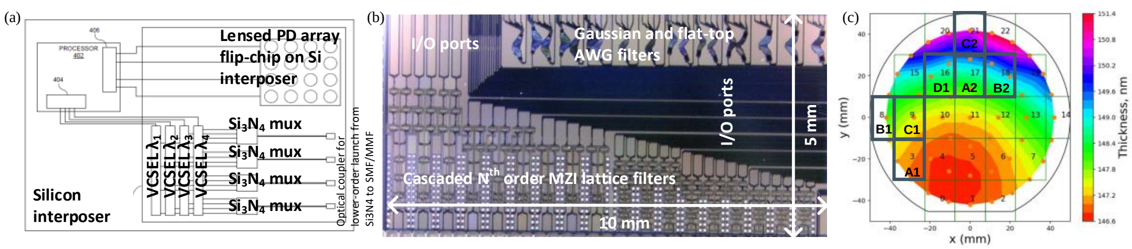

Fig. 1. Optical transceiver module which consists of 4 main parts: 1. low noise, single-mode, polarization locked VCSELs, 2. Si_3N_4 multiplexer into lower order mode launch into SMF/MMF array, 3. Lensed photo-detector (PD) array, 4. Zig-zag de-mux from SMF/MMF array, (b) tape-out of Si_3N_4 chip, (c) wafer thickness uniformity and die locations: A1, B1, C1, D1, A2, B2, C2.

2. Design and Measurement Results

The Si_3N_4 thickness is fairly uniform with a mean thickness of $\mu_{thickness}$ = 148.2 nm and a standard deviation of $\sigma_{thickness}$ = 2.3 nm as shown in Fig. 1 (c). The reported critical dimension (CD) values are μ_{width} = 238 nm and σ_{width} = 13 nm. It is critical to understand the process variability on device performance from a design standpoint. Phase sensitive (de-)multiplexers like AWGs and lattice filters can be sensitive to phase errors and are dependent on variations in waveguide width (Δw), thickness (Δt), and refractive index non-homogeneity. The change in resonant wavelength can be determined by the following equation: $\Delta\lambda_0 = (\lambda_0 / n_g)\sqrt{(dn_{eff}/dw \cdot \Delta w)^2 + (dn_{eff}/dt \cdot \Delta t)^2}$. By taking into account the group index (n_g) defined as $n_g = n_{eff} - \lambda_0 \cdot dn_{eff}/d\lambda$, the resonant wavelength shift $\Delta\lambda_0$ for each dimensional variation can be calculated by the following: $\Delta\lambda_0 / \Delta w = (\lambda_0 / n_g)(dn_{eff}/dw)$ and $\Delta\lambda_0 / \Delta t = (\lambda_0 / n_g)(dn_{eff}/dt)$. In Fig. 2 (a) – (b), n_{eff} and n_g monotonically increase as waveguide dimensions increase because modal confinement is larger within the Si_3N_4 material. It also turns out that width and thickness sensitivity on the effective index are de-coupled when the width > 800 nm and thickness > 300 nm. The single-mode waveguides used throughout this paper have dimensions: 150 nm x 1000 nm and exhibit n_{eff} variations of d_{neff}/dw = 6.396e-5 /nm and d_{neff}/dt = 1.200e-3 /nm. Therefore, starting wafer thickness uniformity is the most critical parameter in controlling phase errors. If we assume, $\sigma_{thickness}$ = 2.3 nm, the expected n_{eff} variation is d_{neff} = 0.0027 which can play a significant role in AWG channel cross talk (*XT*) as shown later. The wavelength shift variations also follow the same trend with $\Delta\lambda_0/dw$ = 0.05 nm/nm and $\Delta\lambda_0/dt$ = 0.804 nm/nm as shown in Fig. 2 (c) – (d). Bends were all kept to R_{min} = 50 μm for a theoretical bending loss = 0.05 dB/180°.

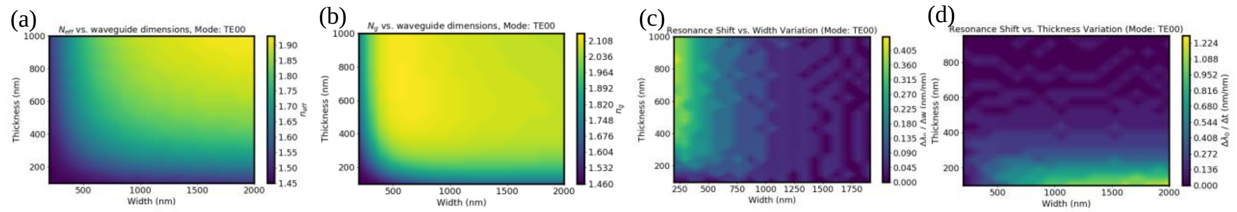

Fig. 2. Finite difference eigenmode (FDE) calculations for (a) effective index (n_{eff}), (b) group index (n_g), (c) wavelength shift vs. width ($\Delta\lambda_0/dw$), (d) wavelength shift vs. thickness ($\Delta\lambda_0/dt$)

The corner case in our wafer map indicates the largest wavelength shift is attributed to thickness variation and will yield $\Delta\lambda_0$ = 1.85 nm, which should not affect CWDM applications significantly. Use of thicker single mode waveguides (800 nm x 800 nm) would significantly reduce thickness variations because of increased modal confinement within the high refractive index region. However, phase errors due to increased photon interaction with sidewall roughness, refractive index inhomogeneity, and film stress will have to be considered as well. The AWGs are designed for a channel spacing = 25 nm with the expectation that the center passbands will be centered at 990, 1015, 1040, and 1065 nm. All TE measured responses shown in Fig. 3 are normalized to a 1 µm wide straight waveguide. The 1 µm wide straight waveguide TE losses were determined to be about 0.3 – 0.4 dB/cm at λ = 1065 nm from a series of cutback test structures. The best performing device came from die C2 and has a *XT* < -35 dB with insertion losses (*IL*) < 1 dB for all 4 channels. Peak passband variation of the measured AWGs over 7 dies are shown.

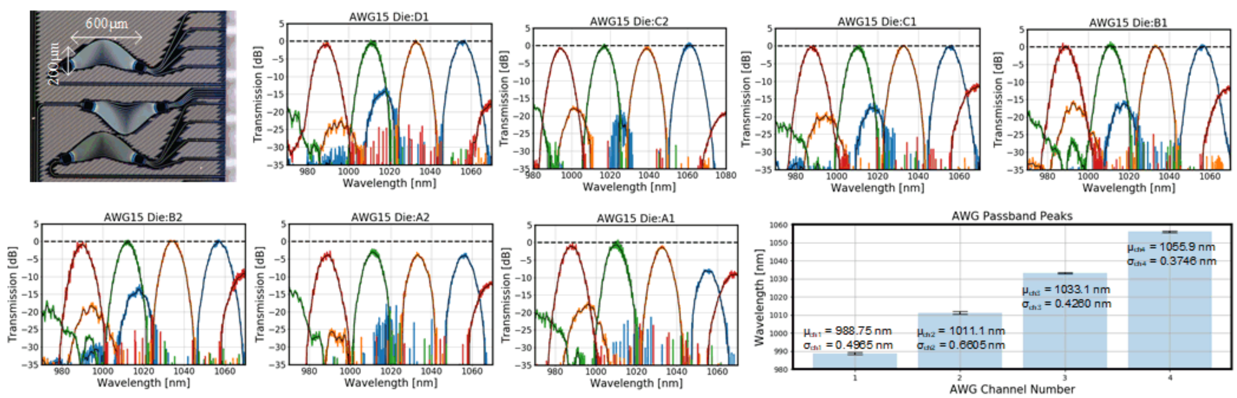

Fig. 3. Measured 1 x 4 Gaussian AWG (de-)mux spectrum across 7 dies. AWG footprint ~ 200 x 600 µm. Peak passband wavelength variation for channels 1- 4 over 7 dies. Mean passband peaks are 988.75, 1011.1, 1033.1, 1055.9 nm, with a separation of 22.3, 22.0, and 22.8 nm.

Transmission loss in Gaussian AWGs increases rapidly from each center peak passband. Therefore, tight restriction is placed on operating temperature and the laser wavelength tolerance. The Si_3N_4 Gaussian AWGs in this paper experience passband shifts ~ 1.052 nm at T = 80 °C, with an incurred loss of ~ 0.2 dB. The 1065 nm VCSELs developed at HPE [1] have a shift of 70 pm/ °C and precludes the use of a Gaussian AWG for operating temperatures up to 80°C unless thermal tuning or laser tuning is implemented, which further increases the power consumption.

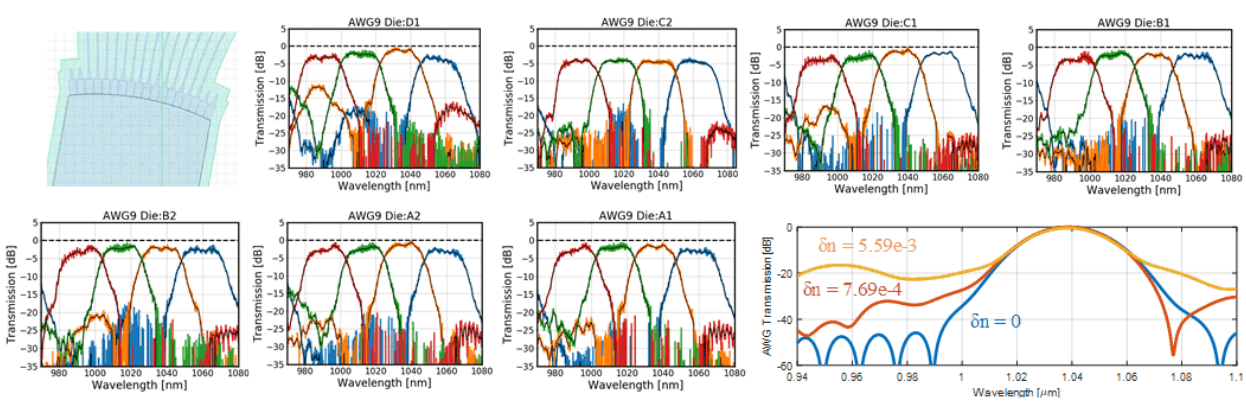

Fig. 4. Measured 1 x 4 flat-top AWG (de-)mux spectrum across 7 dies and mask layout of FPR region with MMI apertures (W_{mmi} = 4 µm, L_{mmi} = 8 µm, W_{taper} = 2 µm, L_{taper} = 6 µm). Simulation of index variation/phase errors on AWG *XT*

As a result, flat-top AWGs were designed to accommodate the power-penalty from high temperature operation. The flat-top spectrum is realized by imaging a flat electric field at the output plane of the AWG with multi-mode interferometers (MMI) [2]. We do this by carefully optimizing the MMI width and length such that the field distribution is flat enough without incurring a spectral dip as seen in designs with wide widths. The MMI used in our designs has dimensions of W_{mmi} = 4 µm, L_{mmi} = 8 µm. The waveguides feeding in/out of the MMI were linearly tapered from W_{taper} = 1 to 2 µm with a length of L_{taper} = 6 µm. The purpose of the taper is to reduce back reflections going in/out to the MMI. The AWG design itself is the same as the Gaussian AWG, except for the MMI apertures at the I/O plane of the FPR regions. The best performing device are from die C1, B1, B2, A1, and A2 with *XT* < -20 dB at the center of the passband as shown in Fig. 4. *IL* can range from 2 – 4 dB for all 4 channels.

Cascaded MZI lattice filters have shown to be a low loss alternative to realizing flat-top CWDM (de-)muxes [3], [4]. For the CWDM bandwidths involved, it is important to take into account the dispersion of the coupling coefficient κ, and group index n_g. We have implemented 3 different designs as illustrated by Fig. 5 (a) – (b) and the corresponding design parameters are Design 1, 2: $\Delta L_1, \Delta L_2, \Delta L_3$ = 11.44, 5.86, 5.72 µm, $\kappa_1, \kappa_2, \kappa_3$ = 0.50, 0.29, 0.08, and Design 3: $\Delta L_1, \Delta L_2, \Delta L_3$ = 11.44, 5.86, 5.72 µm, $\kappa_1, \kappa_2, \kappa_3, \kappa_4$ = 0.50, 0.29, 0.19, 0.025. The theoretical transmission of each channel are calculated by cascading transfer matrices according to the path taken through the filters. Fig. 5 (a) shows the measured 2-stage 2nd order MZI lattice filter transmission spectra. The spacing between channels 1 – 4 is approximately 23.19, 26.6, and 26.81 nm. The progressively larger *FSR* is mainly due to reduced n_g for longer wavelengths and theoretical *FSR* values show 24, 26, and 27 nm which isn't too far from measured values. Another interesting trend is that the passband width $\Delta\lambda$ increases for longer wavelengths due to coupler and path length dispersion. Fig. 5(b) shows the measured spectra of the cascaded 2-stage 3rd order MZI lattice filter and that further suppression of unwanted *XT* is achieved. The *XT* is significantly improved with measured values of -22.96, -25, -21.28, and -13.65 dB for channels 1 – 4. The loss spectrum gradually increases from the central passband indicating the normal directional couplers are more dispersive than what is simulated, however, *IL* at the central band of 1020 nm is < -1 dB. This can be remedied by designing appropriate broadband directional couplers.

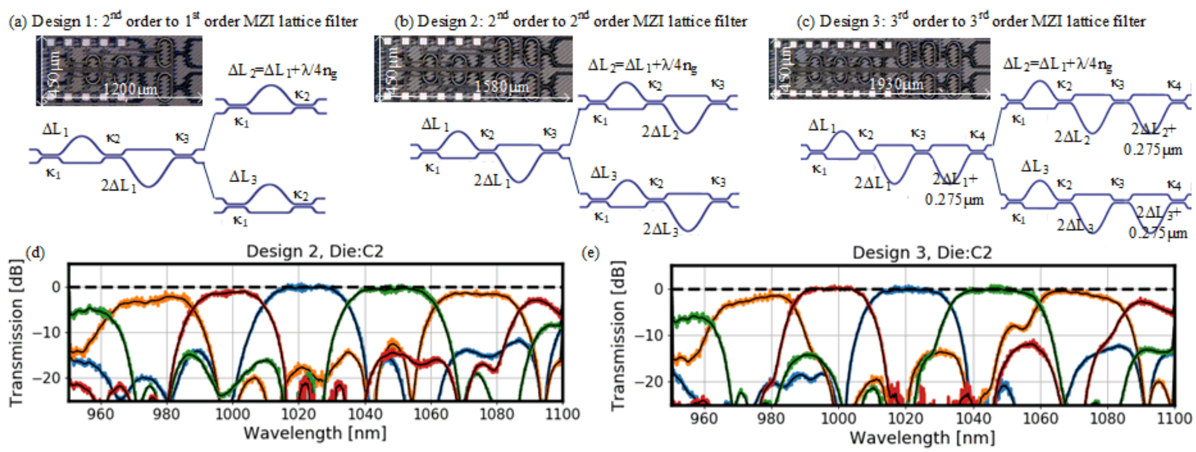

Fig. 5. 1 x 4 (de-)mux MZI lattice filter designs for (a) Design 1, (b) Design 2, (c) Design 3. Measured 1 x 4 (de-)mux MZI lattice filter spectrum for (d) Design 2 and (e) Design 3. Temperature shifts from T = 25 – 80 °C revealed a passband shift of $\Delta\lambda/\Delta T$ ~ 14.5 pm/°C.

3. Conclusion

For Si_3N_4 Gaussian AWGs, we demonstrate *XT* < -35 dB at a peak transmission band with *IL* < 0.5 dB. Measurements were performed over many dies, and pass-band standard deviations for channel 1 – 4 are 0.49, 0.66, 0.42, and 0.37 nm respectively. Results for flat-top AWGs indicate X*T* < -20 dB with *IL* < 3 dB for the best devices. Flat-top cascaded 2nd order and 3rd order MZI lattice filters show a minimum of *XT* < -15 dB and < - 20 dB respectively. The pass-band temperature shift was determined to be 14.5 pm/ °C, which is lower than reported values for silicon. We believe the Si_3N_4 platform has potential for its use in CWDM and possibly DWDM transceiver/optical-modules for data/computer communication in high temperature environments up to 80 °C.

[1] M. R. T. Tan *et al.*, "Universal Photonic Interconnect for Data Centers," *J. Lightwave Technol.*, vol. 36, no. 2, pp. 175–180, Jan. 2018.
[2] S. Pathak, M. Vanslembrouck, P. Dumon, D. V. Thourhout, and W. Bogaerts, "Optimized Silicon AWG With Flattened Spectral Response Using an MMI Aperture," *Journal of Lightwave Technology*, vol. 31, no. 1, pp. 87–93, Jan. 2013.
[3] J. C. Mikkelsen, A. Bois, T. Lordello, D. Mahgerefteh, S. Menezo, and J. K. S. Poon, "Polarization-insensitive silicon nitride Mach-Zehnder lattice wavelength demultiplexers for CWDM in the O-band," *Optics Express*, vol. 26, no. 23, p. 30076, Nov. 2018.
[4] H. Xu and Y. Shi, "Flat-Top CWDM (De)Multiplexer Based on MZI With Bent Directional Couplers," *IEEE Photonics Technology Letters*, vol. 30, no. 2, pp. 169–172, Jan. 2018.